Unsaturated Flow through a Small Fracture–Matrix Network: Part 1. Experimental Observations

T. R. Wood,* R. J. Glass, T. R. McJunkin, R. K. Podgorney, R. A. Laviolette, K. S. Noah, D. L. Stoner, R. C. Starr, and K. Baker

ABSTRACT

The behavior of unsaturated flow was investigated in a laboratory model. A constant and uniform supply of chemically equilibrated water was introduced to the upper surface of three artificial fractures in a surrogate fracture network consisting of a thin wall of uncemented limestone blocks. Water was collected from the lower boundary via fiberglass wicks placed at the bottom of each artificial fracture. Eight experiments were conducted to evaluate the repeatability of flow under nearly identical conditions and to characterize general patterns in flow behavior. Collected data revealed that flow generally converged to a single fracture in the bottom row of blocks. Periods of pathway switching were observed to be more common than periods with steady, constant flow pathways. We noted the importance of fracture intersections for integrating uniform flow and discharging a "fluid cascade," where water advances rapidly to the next capillary barrier creating a stop and start advance of water through the network. Under very similar initial moisture and boundary conditions, flow in the system was less repeatable than expected. The results of this simple experiment suggest that the interaction of multiple fracture intersections in a network creates flow behavior not generally recognized in popular conceptual and numerical models, (i.e., convergence of flow, pathway switching, and fluid cascades).

Several recent government reports have identified shortcomings in techniques available for predicting the transport of contaminants in the subsurface, particularly in the vadose zone (NRC, 2000; GAO, 1998). In the context of unsaturated fracture rock, these shortcomings are often attributed to spatial and temporal heterogeneity and the inability of volume-averaged modeling approaches to adequately represent the full range of dynamical behavior (Wood et al., 2000a). For the past decade, the USDOE has supported field-scale experiments at the Idaho National Engineering and Environmental Laboratory (INEEL) to better understand the flow of fluids and contaminants through fractured basalt vadose zones with the goal of improving predictive models (Wood and Faybishenko, 2000; Faybishenko et al., 2001). Field experiments began in 1993 and 1994 with the INEEL Large Scale Pumping and Infiltration Tests (Wood and Norrell, 1996; Wood et al., 1997), the Analog Site for Fractured Rock Characterization, 1995 through 1997 (Faybishenko et al., 1998, Faybishenko et al., 2000), and the Hell's Half Acre Basalt Infiltration tests, 1997 through 2000 (Wood and Podgorney, 1999; Podgorney et al., 2000; Wood et al., 2000b). These tests were conducted at the 100-, 10-, and 1-m scales, respectively. Due to the very different behavior observed at these different scales, it can be concluded that fractured basalt vadose zone must be conceptualized at a hierarchy of scales (Faybishenko et al., 2001). Although the hierarchy of scales approach describes behavior of a fractured basalt vadose zone at multiple scales of observation, it fails to provide a means for scaling between scales of observation and does not describe the unit processes generating flow dynamics observed during field testing.

Common to this conceptualization, and indeed to other studies conducted on a wide variety of fractured rock types, is the suggestion that at large spatial scales and relatively short temporal scales, fracture networks can facilitate the deep penetration of dissolved contaminants, even when the rock matrix is far from saturation (e.g., Fabryka-Martin et al., 1996; Davidson et al., 1998; Dahan et al., 1999; Faybishenko et al., 2000; Wood and Norrell, 1996; Podgorney et al., 2000; Wood et al., 1997, 2000a, 2002b, 2002c; Glass et al., 2002a, 2002b; Nicholl and Glass, 2002). Mechanistically, the behavior of individual fractures must organize to yield this large-scale behavior. To consider this issue, Glass et al. (1995, 1996) assembled understanding at the single fracture–scale and then proposed via a thought experiment that fracture intersections behaving as capillary barriers might cause both the confluence and sequestration of flow within a fracture network to create large-scale gravity-driven vertical pathways even in the absence of significant vertical heterogeneities (e.g., vertical faults).

As a next step toward understanding how existing models should evolve to make better predictions of fluid flow in fracture networks at the field scale, a comparison is needed between the behavior of flow in a fully characterized fracture network to modeled behavior using standard approaches. The similarities and differences between the observed and the predicted behaviors will serve to show what works and what does not when conventional modeling approaches are applied to unsaturated flow in a fractured rock network. We focus on this comparison in two companion papers. This paper, Part 1, describes the experimental data set collected for comparison to equivalent continuum modeling simulations described in Part 2 (Fairley et al., 2004). Our objectives are (i) to better understand phenomena that

T.R. Wood, T.R. McJunkin, R.K. Podgorney, R.A. Laviolette, K.S. Noah, D.L. Stoner, R.C. Starr, and K. Baker, Idaho National Engineering and Environmental Laboratory, P.O. Box 1625, Idaho Falls, ID 83415-2107; R.J. Glass, Sandia National Laboratories, P.O. Box 5800, Albuquerque, NM 87185. Received 14 May 2003. Special Section: Understanding Subsurface Flow and Transport Processes at the Idaho National Engineering & Environmental Laboratory (INEEL) Site. *Corresponding author (tqw@inel.gov).

Published in Vadose Zone Journal 3:90–100 (2004).

677 S. Segoe Rd., Madison, WI 53711 USA

Abbreviations: INEEL, Idaho National Engineering and Environmental Laboratory.

influence dynamical behavior of unsaturated flow in fractured rock networks and (ii) to collect a data set with sufficient control and resolution for comparison to numerical simulations.

We constructed the simplest fracture network that would satisfy our objectives. The experimental work by Glass et al. (2002a), where stacked bricks formed a small network, led us to conduct a similar experiment using natural rock and distributed input. Our initial results, summarized by LaViolette et al. (2003), showed that flow tended to converge in this simple analog fractured rock network even under conditions of distributed uniform flux, supporting the conjecture of Glass et al. (1995, 1996) that fracture intersections exert a first-order control on unsaturated flow at the network scale by acting as local capillary barriers that focus flow. Here, we provide the complete experimental design and give full details of experimental results used for modeling described in Part 2 (Fairley et al., 2004). Because of the similarity in our approach, we will necessarily echo some of the findings of Glass et al. (2002a), such as intersections acting as capillary barriers, flow switching, and pulsation along pathways, but our work has the following differences: (i) distributed flow to multiple fractures, (ii) natural rock, (iii) different boundary condition, and (iv) multiple realizations of reasonable duration. Taken as a whole, these studies identify several critical issues that require further study regarding the application of popular modeling approaches to unsaturated flow in fractured rock.

EXPERIMENTAL DESIGN

Our needs required that the experimental parameters and natural properties (e.g., fracture aperture, matrix porosity, mass flux) be accurately known to understand the fundamentals controlling flow behavior for input to models. As a result, we designed and conducted a series of experiments, using an analog fracture–matrix network made of limestone blocks stacked into an uncemented wall. The joints between adjacent blocks represent fractures and the limestone blocks represent a rock matrix. We wished to avoid unnecessary disturbance to the system that might affect dynamical behavior, so we designed and built an automated system that acquired and processed inflow, outflow, and photographic data during each of the tests. The experimental system provided continuous testing for days at a time without human intervention.

Experimental System

The experimental apparatus consisted of a frame to hold the blocks in place, a water inflow and outflow system, laboratory scales or weighing load cells for tracking mass in and out and time-lapsed photography. Several materials were considered for use during these tests. Our selection criteria included: (i) a relatively homogeneous permeability and porosity field, (ii) a rock easy to shape and durable during handling, and (iii) a rock that visually showed wetting for photographic imaging. We selected a building stone, which is a fine-grained dolomitic limestone from the Ordovician Oneota formation, quarried in Le Sueur County, Minnesota (Vetter Stone Company). Hydraulic tests on representative samples (Table 1) yielded average values for porosity of 15% (±1.5%) and permeability of 1.3×10^{-15} m^2 (saturated hydraulic conductivity, K_s, of 7×10^{-5} cm min^{-1} at 21°C) (Table 1). Twelve blocks were cut to size with the nominal dimensions of 5 by 7 by 30 cm for testing. Asperities were minimized with sandpaper. The block surfaces were washed thoroughly and then assembled into the model without contaminating the fracture surfaces.

Table 1. Measured permeability and porosity dolomitic limestone building stone.

Flow direction	Core sample†	Porosity	Permeability
		%	m^2
Horizontal X	A	17.1	2.5E-15
	B	15.0	1.1E-15
	C	15.8	8.9E-16
	Average	16.0 ± 0.9	1.5E-15
Horizontal Y	A	16.4	1.1E-15
	B	12.4	5.9E-16
	C	15.7	2.4E-15
	Average	14.9 ± 1.6	1.3E-15
Vertical Z	A	14.9	1.4E-15
	B	12.5	7.9E-16
	Average	13.7 ± 1.2	1.1E-15
All directions	Average all	15.0 ± 1.5	1.3E-15

† All these samples were drilled from the same piece of limestone. Porosity is a rock property that is isotropic; therefore, differences in porosity are not directional and are indicative of the variability of the rock as a whole.

The blocks were stacked on end, four blocks wide by three blocks high, forming a wall 91 cm high, 28 cm wide, and 5 cm thick. Figure 1 is a schematic representation of the system and shows the labeling scheme for the blocks and fractures. The resulting surrogate fracture network had three vertical fractures (labeled V1, V2, and V3) and two horizontal fractures (labeled H1 and H2). Since the blocks were pressed together under lateral pressure, they had some contact area within each fracture and the resultant aperture field exhibited some variability, which was measured for each model. The measured apertures for all models of the vertical fractures ranged from 0.030 to 2.5 mm, and those of the horizontal fractures ranged from 0.025 to 3.2 mm. Where four blocks came together, an intersection was formed with additional irregularities due to imperfections along the corners of the blocks, which generally acted to increase the aperture size at the intersection. The entire system was encased in transparent plastic to reduce evaporation.

The water used for the tests was tap water (groundwater) equilibrated with crushed limestone and then filtered through a 0.2-μm membrane. Equilibrated water was applied to the top of each fracture across the width of the fracture through fiberglass wicks. At the bottom of each vertical fracture, a fiberglass wick carried water to a bottle either setting on a laboratory balance or suspended from a weighing load cell. Thus, a total of six bottles (three inflow and three outflow) were used to measure the mass in and mass out for the three vertical fractures. The resolution of the mass flux was ±0.1 g, and the mass was recorded at 10-s intervals. The presence of bacteria in the influent and effluent was monitored using direct cell counts. Samples were taken daily from the discharge bottles, stained, and observed microscopically. Using these techniques, microbial numbers in the test system were determined to remain near background. Automated time-lapsed photographs were taken to track the progress of the wetting front. Fluorescent lighting was used to supplement the overhead laboratory lighting.

Experiments Conducted

A total of eight experiments were conducted. We conducted three different types of tests: (i) random stacking of blocks (Tests 1–3), (ii) a planned stacking of blocks to focus discharge

Table 2. Summary of experiments.

Test number	Type	Comments
1	Random	Oven dried, uniform discharge, bottles overflowed at 48 h
2	Random	Oven dried, convergent flow for first 2000 s, uniform flow thereafter, complete data set
3	Random	Oven dried, convergent flow, complete data set
4	Designed stack	Oven dried, convergent flow, pathway switching, complete data set
5	Constant stack	Oven dried, convergent flow, complete data set
6	Constant stack	Dried in place, convergent flow, complete data set
7	Constant stack	Dried in place, convergent flow, complete data set
8	Constant stack	Dried in place, convergent flow, lost discharge data

to a particular outlet (Test 4), and (iii) repeated tests using the same stack of blocks (Tests 5–8). For all tests, mass flux and points of entry to the model were kept the same (i.e., constant, uniform flux, identical source locations, and a nominal 72-h test duration). In Tests 5 through 8 we tilted the experiment slightly forward to ensure that water ran within the fractures toward the side where we recorded the wetting history via time lapsed photography. Table 2 summarizes the tests. In the following, we describe each test in detail.

In Tests 1 through 3, after oven drying, the bricks were stacked so that bricks adjacent in one test were not adjacent in subsequent tests. Imperfections in the bricks, caused by saw marks, geometry of cuts, or chips resulted in variations of the aperture field. A feeler gauge, consisting of thin metal blades of known thickness, was used to measure the aperture field for each test by inserting the blades of the feeler gauge into the fractures at intervals of 2.5 cm and recording the thickness required to make contact with both surfaces of the fracture. In Test 4, thin metal shims (0.5 mm) placed at edges of the fractures were used to control the aperture field in an attempt to focus discharge to the lower right-hand fracture. It was reasoned that capillary forces controlled flow in the system. Thus, by creating large apertures in the lower left corner of the model, flow would be forced toward the lower right corner. Four shims in each fracture were inserted 0.5 cm into the vertical fractures V1 (between Blocks A1 and A2, and B1 and B2) and V2 (between Blocks A2 and A3) and in the horizontal fracture, H2 (between B1 and A1, and B2 and A2) (depicted as bold lines in Fig. 1).

In Test 6 we wanted to evaluate the repeatability of the advance of the wetting front and determine if dynamical behavior occurred at the same elapsed time and same location in the same aperture field starting from similar initial moisture conditions. The blocks were initially oven dried and then stacked into place in Test 5. The bricks remained in place in the frame for Tests 6, 7, and 8 because it was impossible to remove the bricks, dry them, and restack them so that the aperture field was identical to a previous test. We air dried the blocks in place using a fan to force air through the model until reaching a target electrical resistance measured across electrodes at the side bricks. We employed a stainless-steel bolt, drilled and then threaded 1 cm into the blocks on the outside edge of the model, to increase the contact area and reduce the possibility of surface drying of the blocks dominating the resistivity reading. In cases where the electrical resistance became too low, we used a humidifier to raise the moisture content of the bricks, thus lowering the resistance to the target level.

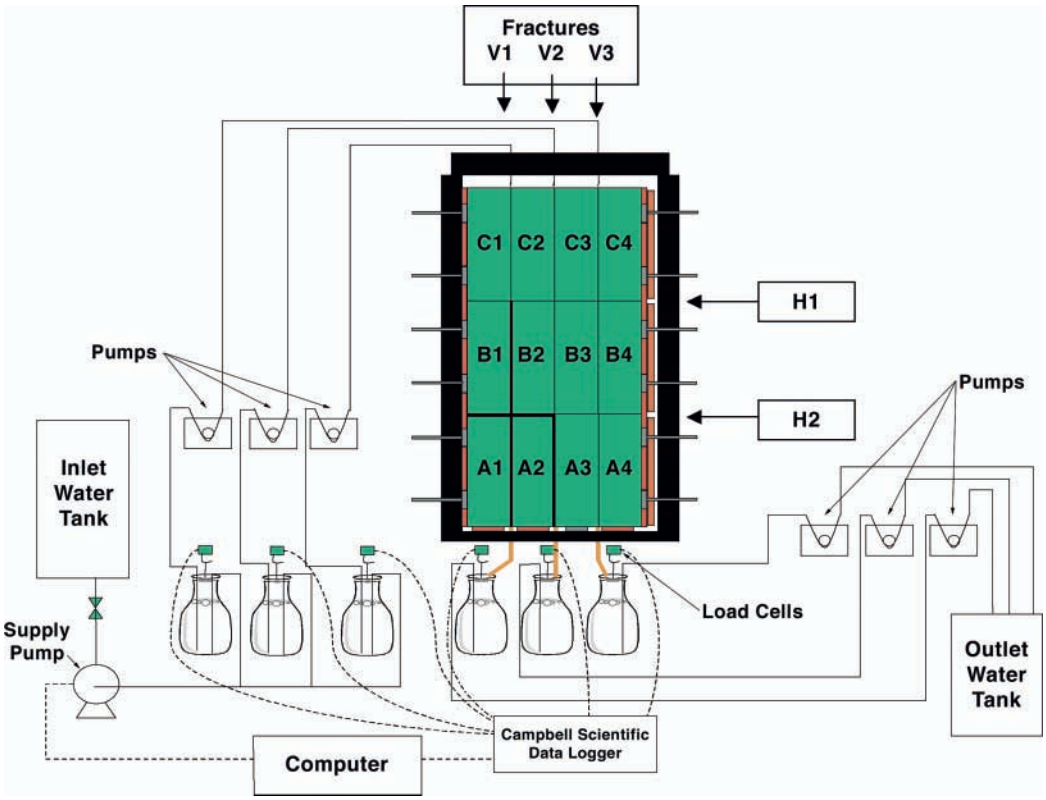

Fig. 1. Schematic of set up for 12 block experiments. The fractures held open with shims in Test 4 are highlighted with bold lines.

Near the end of Test 1, the automated system for emptying the discharge bottles failed at an elapsed time about 48 h. For Test 1, all of the discharge data are presented and the unusable data noted. During Test 8, a malfunction of the water collection system caused the program collecting the discharge data to crash, preventing the use of any discharge data for Test 8. However, the visual image sequence is usable and these images are analyzed and presented in a later section.

RESULTS

Flow Monitoring Data

A constant and continuous flux of 1 mL min^{-1} was added to the top of each fracture for the duration of all tests. This was verified with laboratory scales or weighing load cells on the input side of the apparatus. No significant variations in the rate of flux for each of the three fractures were observed during any of the eight tests. Figure 2 shows the discharge rate by fracture vs. time for Tests 1 through 7. Spikes in the data for Tests 2 through 4 (e.g., Test 2, elapsed time ≈2000 min) are caused by the routine calculating the flow rate from the mass of the discharge bottle and are not real events. When the bottles were emptied by the automated system it created a spike in calculated flow rate. Load cells were used for Tests 5 through 8, which are inherently noisier than scale data. We processed the data with the same smoothing routine used in Tests 1 through 4. The smoothing routine was a hamming window (i.e., weighted average) of 31 data points centered on the mass measurement being smoothed. The differences of consecutive smoothed mass data points were divided by the time interval between measurements to compute a flow rate in grams per minute. Additionally, the data were smoothed by omitting spikes and using larger symbols to visually reduce the appearance of noise caused by the weighing load cells.

In most tests there was a tendency for the discharge flow to converge with depth. We defined convergence for the purposes of this experiment as greater than one-half of the total flow discharging to a single fracture. Of the five configurations tested from initially oven-dried conditions (Tests 1–5), three displayed convergence at the scale of the experiment. (Tests 3, 4, and 5 show convergence; Test 2 shows convergence until elapsed time 2000 min.) The configuration of Test 5 was tested three more times after air drying to similar moisture content (Tests 6 and 7 plotted in Fig. 2; Test 8 outflow data was lost). The outflow data of Test 6 and 7 show similar convergence, with an increasing amount of flow going to the middle fracture, V2. Even with only five independent samples (corresponding to the five permutations of the blocks), a quantitative estimate of the uncertainty in the mean occurrence of converging flow can be achieved via the bootstrap method (Efron and Tibshirani, 1993). The bootstrap with exact enumeration gives (3 + 1)/5 for the mean occurrence of converging flow at the 80% confidence level. Therefore, the occurrence of converging flow is at least as statistically significant as the occurrence of uniform flow in these experiments.

In Test 4, we constructed the model using shims placed at the edge of the bricks so that wider apertures were in the lower left-hand corner as mentioned above. The intent was to see if we could force water to the lower right fracture. We thought that capillary forces probably controlled flow; thus fracture flow would preferentially occur in narrower fractures. As can be seen in Fig. 2, flow for about the first 120 min of the experiment did go almost exclusively to the right-hand fracture. An abrupt switch in flow occurred at approximately 120 min, and then most of the flow went to the left-hand fracture for the remainder of the test. There are at least two possible explanations for this abrupt switch. The first is that imbibition by the matrix during the first 120 min reduced flow through the fractures and thus capillary forces dominated within the fractures at early time. However, with increasing time, imbibition was reduced, flow within the fractures increased, and gravitational forces became more important. This change in relative influence of capillary and gravitational forces caused a switch in the flow path to the left-hand fracture by allowing a critical capillary barrier to be breached. A second explanation could be that with time, the critical capillary barrier simply wetted and was breached due to a reduction in the local contact angle. In this case, the expectation is that the wetting of the surrounding matrix reduces the effective contact angle from the unwetted rough surface.

We observed many instances of pathway switching where discharge from one fracture would increase at the expense of another. Examples of flow path switching can be seen to varying degrees in all tests. The switching of flow from one pathway to another occurred either gradually in intervals of hundreds of minutes or abruptly in a period of a few minutes. An example of gradual pathway switching can be seen in Test 3; beginning at an elapsed time of approximately 3800 min flow gradually shifts from V1 to V2 during the next 2000 min. Discharge to V3 remains constant. An abrupt sudden shift can be seen in Test 4 at an elapsed time of approximately 2800 min when discharge to V2 suddenly ceases and flow switches to V1. During the next 1400 min the discharge gradually switches back to V2 at the expense of V1. Examination of the outflow plots in Fig. 2 indicates that regimes of pathway switching (either gradual or abrupt) are more common than periods of steady, constant flow to the discharge points. Only about 10 000 min of the approximately 25 000 min of testing data presented in Fig. 2 represent periods of relatively steady, constant flow to the discharge points. The other 15 000 min of data are periods with either abrupt or gradual pathway switching.

We cannot explain the causes of the pathway switching with the data set we collected. The boundary conditions of temperature, air pressure, and initial moisture content were not controlled or monitored sufficiently to correlate to pathway switching. We speculate that subtle changes in temperature, air pressure, or vibrations may trigger some of the switching events. Others may be the result of the complicated interaction of gravity, capillary, and inertial forces that develop in the

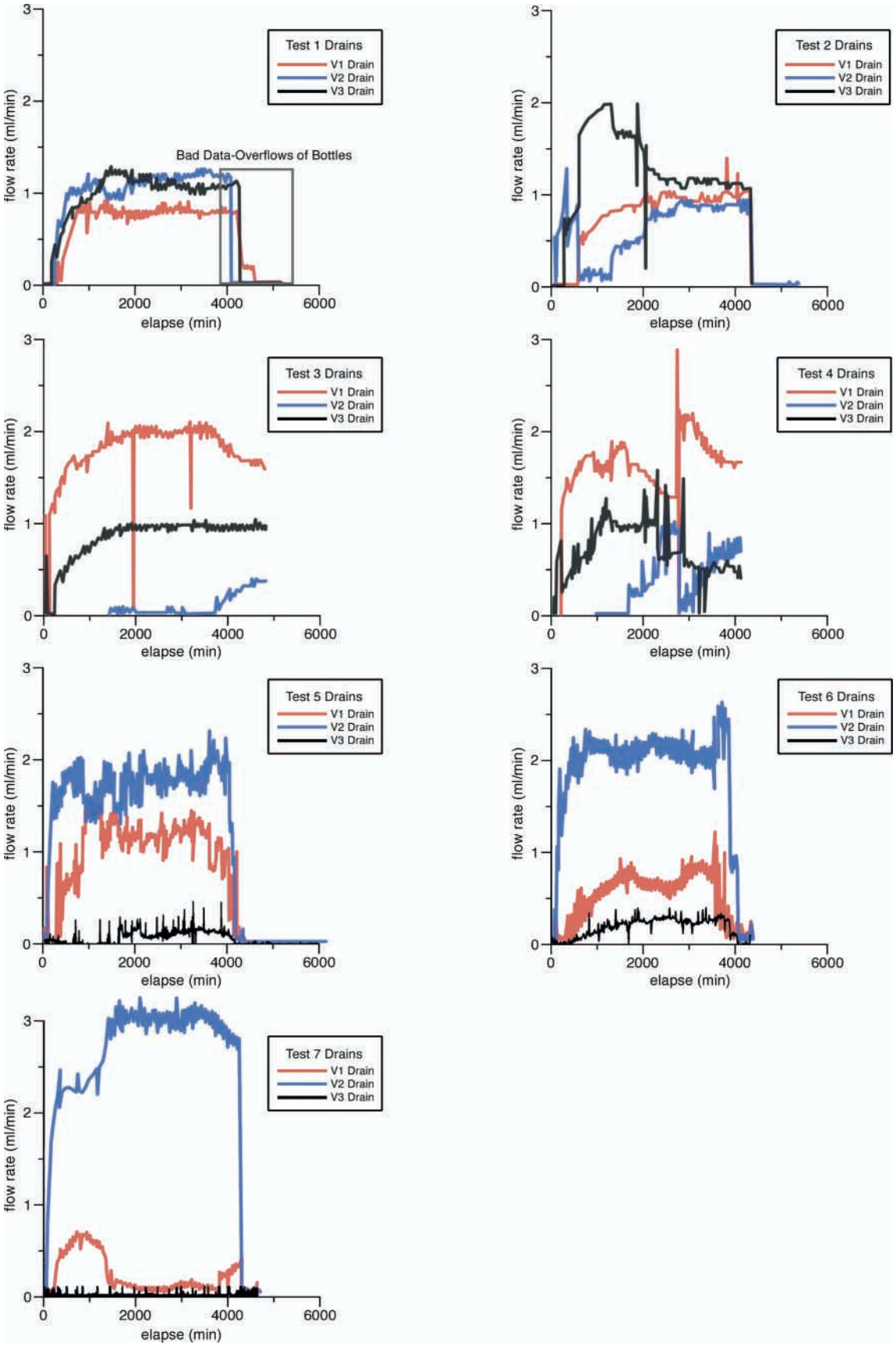

Fig. 2. Plot of discharge flux in milliliters per minute for Fractures V1, V2, and V3 for Tests 1 through 7.

fracture network. Our data corroborate observations made by Glass et al. (2002a) in an experiment with better control and monitoring of air pressure, humidity, and temperature. In their experiment, some pathway switching was explained by a simple evaporation–condensation mechanism, while other pathway switching could not be explained. They concluded that fluctuations in the outflow occur spontaneously within the fracture network and speculated that pulsation at fracture intersections along flow pathways might be the cause of flow path switching. Our experiments confirm that flow path switching appears to be a common characteristic of unsaturated flow in fracture networks.

Time Lapse Imaging

The time-lapse images provide a qualitative record of the advance of the wetting front through the fracture network. A shortcoming of this experimental setup is that the model is not truly two-dimensional—some flow also occurred back of the front face of the block wall and was not recorded with time-lapsed photography because we could not photograph the back of the block wall. However, to alleviate this problem somewhat, we tilted the frame slightly forward in Test 5 through 8 to enhance viewing of the wetting front. Figure 3 shows a side-by-side comparison for Tests 5 through 8 at times of 7 min 30 s, 22 min 49 s, 50 min 17 s, 1 h 47 min, 3 h 39 min, and 10 h 9 min. The wetted areas are dark, and the horizontal dark bands are shadows from the apparatus.

During the first time step for all four tests (Fig. 3), water traversed one or more of the vertical fractures (V1, V2, V3; Fig. 1) to the level of the first horizontal fracture, H1. In Tests 6, 7, and 8, it can be seen that water initially left the fractures and traveled along the face of the model at an off vertical angle. The water remained within the fractures throughout Test 5. It is possible that water left the fracture during the early parts of the test because the initial moisture conditions were wetter in the limestone matrix during the three later tests than in Test 5.

At the second time step the pathway dynamics became more interesting as the water began to spread laterally in the first horizontal fracture (H2). In Test 7, at the second time step, water had traversed the entire fracture network to the terminus of V3. For the other tests, the wetting front is not visible at the lower boundary, although flow may have been arriving at the lower boundary behind the plane of the front surface.

At the third time step, imbibition into the limestone matrix is apparent in the upper row of blocks (Row C) and flow appears to be equal in V1, V2, and V3 in Row C. However, in the second row of blocks (Row B), flow in the fractures tended to converge to one or two of the vertical fractures. The convergence of flow in Row B is more apparent in the fourth time step. Here it can be seen that for Test 5 flow was focused in V2 in Row B, for Test 6 flow as focused in V2 and V3 in Row B, in Test 7 the flow was focused to V1 and V2, and in Test 8 the flow was focused in V2 and V3. It is likely that small differences in initial moisture content, hysteresis, and the fact that the flow is inherently unstable may account for the variation in wetting patterns between tests.

During the last two time steps it can be seen that for all four tests, flow tended to converge into the middle fracture, V2, through the lowest Row A (this is confirmed by outflow data in Fig. 2). Matrix imbibition begins to color the entire block wall and the time-lapsed photographic record is of little use in tracking the flow of water after an elapsed time of about 12 h.

Figure 4 shows the development of the wetted structure for each test, with each color representing wetted structure at each time step from Fig. 3. As described above, water initially left the fractures in Tests 6, 7, and 8 and traveled along the face of the model at an off vertical angle, probably because the initial moisture contents of the bricks were higher in the later tests as a result of their being dried in place. Focusing of flow into the fractures of Row B and Row A and convergence to V2 can be seen in all tests. We note that flow apparently zig-zagged through Row B either going down V2, V2 and V3, or V2 and V1, but it tended to converge in all cases to V2 through Row A. Variation in the pathways through Row B is an example of nonrepeatable, dynamical behavior. Figure 4 also shows the existence of several stalled flowpaths that initially exhibited rapid movement of water, but failed to remain active and dried out as the test progressed. Stalled flow paths can be seen in several tests. In Test 5 along fracture V1 just below H1, the green color stops with only a small advance of yellow and orange. In Test 6 along the lower reach of V3 at the intersection with H2 the green color stops with only a slight advance of yellow and orange. In Test 8 along the lower reach of V1 at the intersection of H2 and in V3 at the bottom of the model the green color stops with no yellow or orange advancing forward. The stalled pathways did not always occur in the same locations during repeated tests.

Several instances were noted where a finger of water rapidly traverses a large vertical distance of a single fracture in a brief period of time. These events, or "fluid cascades," were also documented in the experiment of Glass et al., (2002a). As an example of a fluid cascade, Fig. 5 shows the buildup of water at the intersection of Fractures V3 and H1 and the subsequent fluid cascade down V3 past the intersection with H2. The buildup of water in the horizontal fracture H1 occurred in 1008 s. The resulting fluid cascade traversed 32 cm of V3 in a brief period of time (<26 s between frames of the time-lapse photographic record). The estimated minimum velocity of the fluid cascade is approximately 1.2 cm s^{-1} (32 cm/26 s), which is about two orders of magnitude less than the flow of water calculated assuming saturation and a unit gradient for the measured aperture field.

The graph in Fig. 5 illustrates the advance of the tip of the wetted finger in Fracture V3 vs. time. The fluid cascade appears as a large step at 1447 s. In comparison, during Tests 5 and 7, wetting of the same vertical interval of Fracture V3 occurred only by matric imbibition with no apparent flow in the fracture. In Test 8, water moved

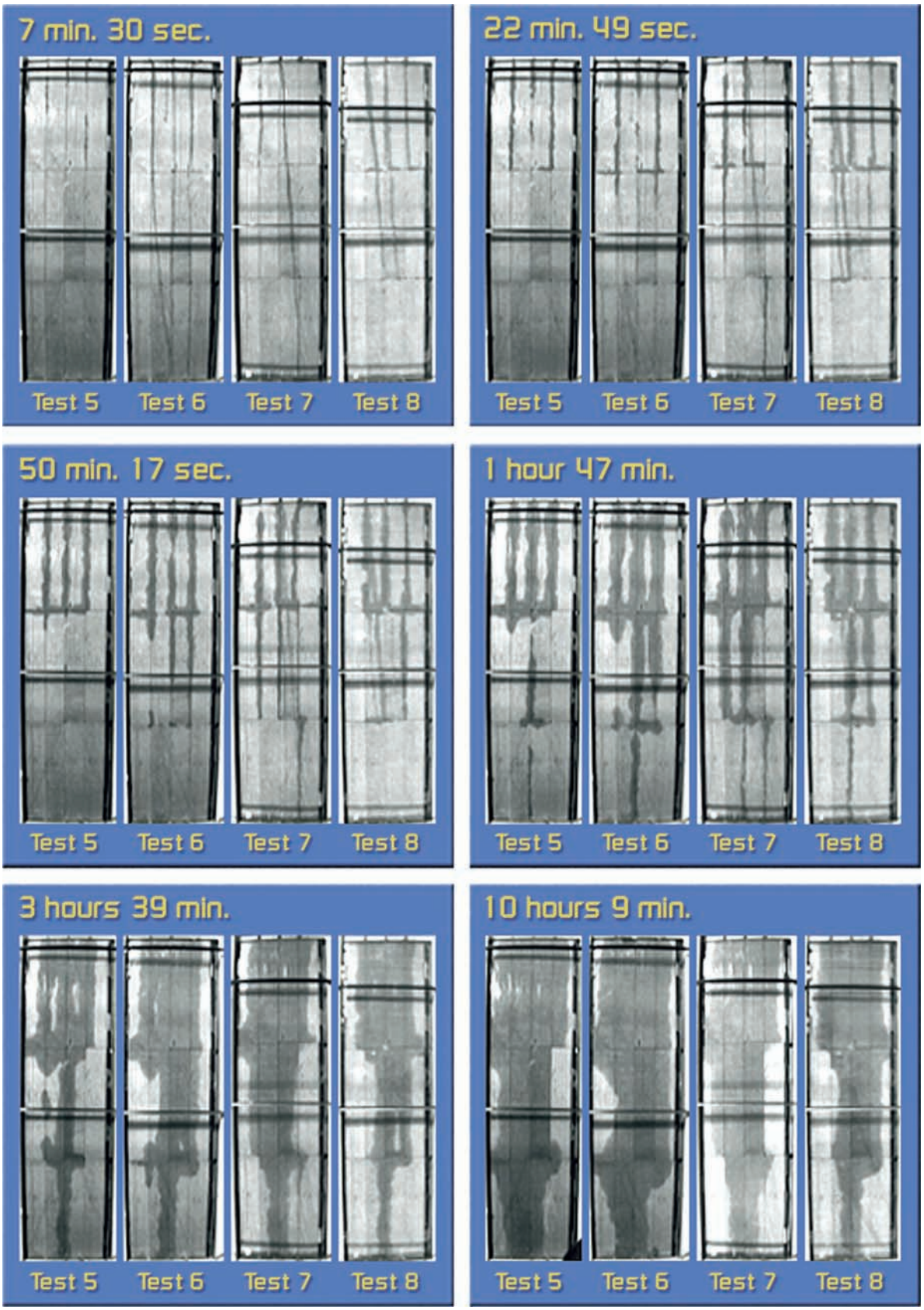

Fig. 3. The photographic images above show the variation in wetting front patterns for tests conducted under nearly identical conditions. For all tests, the boundary conditions remained constant with 1 mL min^{-1} applied via needle to each of the three fractures and outflow carried from each fracture via a fiberglass wick.

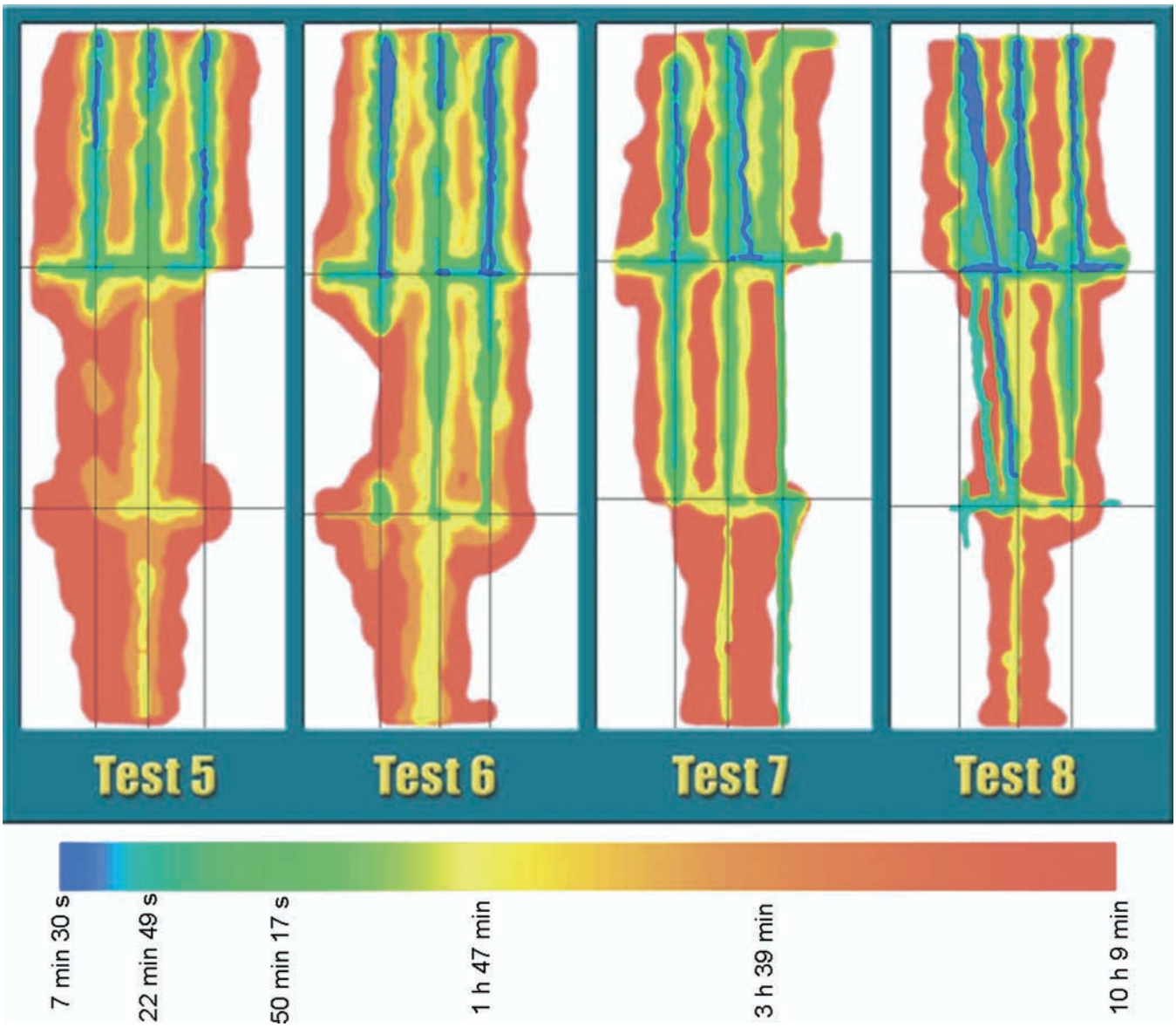

Fig. 4. Comparison of wetted structure development during four tests. The color bar represents the sequence of development in these composite images. Individual colors represent the sequence of development at 7 min 30 s, 22 min 49 s, 50 min 17 s, 1 h 47 min, 3 h 39 min, and 10 h 9 min.

slowly in the same interval of the vertical fracture in 1146 s, at an estimated velocity of approximately 0.03 cm s^{-1} (32 cm/1146 s). The differences in wetting advance through this section of the fracture under nearly identical laboratory conditions underscore the inherent instability of flow in unsaturated fractured rock networks.

Fluid cascades appear to be caused by the pooling above a capillary barrier created at the fracture intersection and the subsequent release of water as gravitational forces breech the barrier. This process of flow integration and subsequent intermittent release at a single fracture intersection has been studied recently by Wood et al. (2002). They noted that water filled the connecting horizontal fracture to create a much larger integration volume than could form only in the pool immediately above the intersection within the fracture. Water entering the pool from above causes pressure to build in the combined pool volume until a critical point is exceeded, after which a cascade ensues, creating a gravity driven finger (e.g., Nicholl et al., 1993; Su et al., 1999). Water then advances rapidly to the next barrier, thus creating a stop and start advance of water through the network. We note that the fluid cascade illustrated in Fig. 5 was not initially captured by the next lower intersection. We attribute this to two factors. First, the capillary strength of the intersection was not sufficient to stop the mass of water plus the inertial forces of the fluid cascade. Second, fluid storage above and in the horizontal fractures to either side was insufficient to attenuate the inertial forces and reduce gravity forces to the point where the capillary barrier could hold the advancing cascade. However, at later times, fluid below the intersection becomes disconnected from the fluid finger, and flow at the intersection is diverted to the left to V2 (see Fig. 3, Test 6, 1 h 47 min). This observation underscores

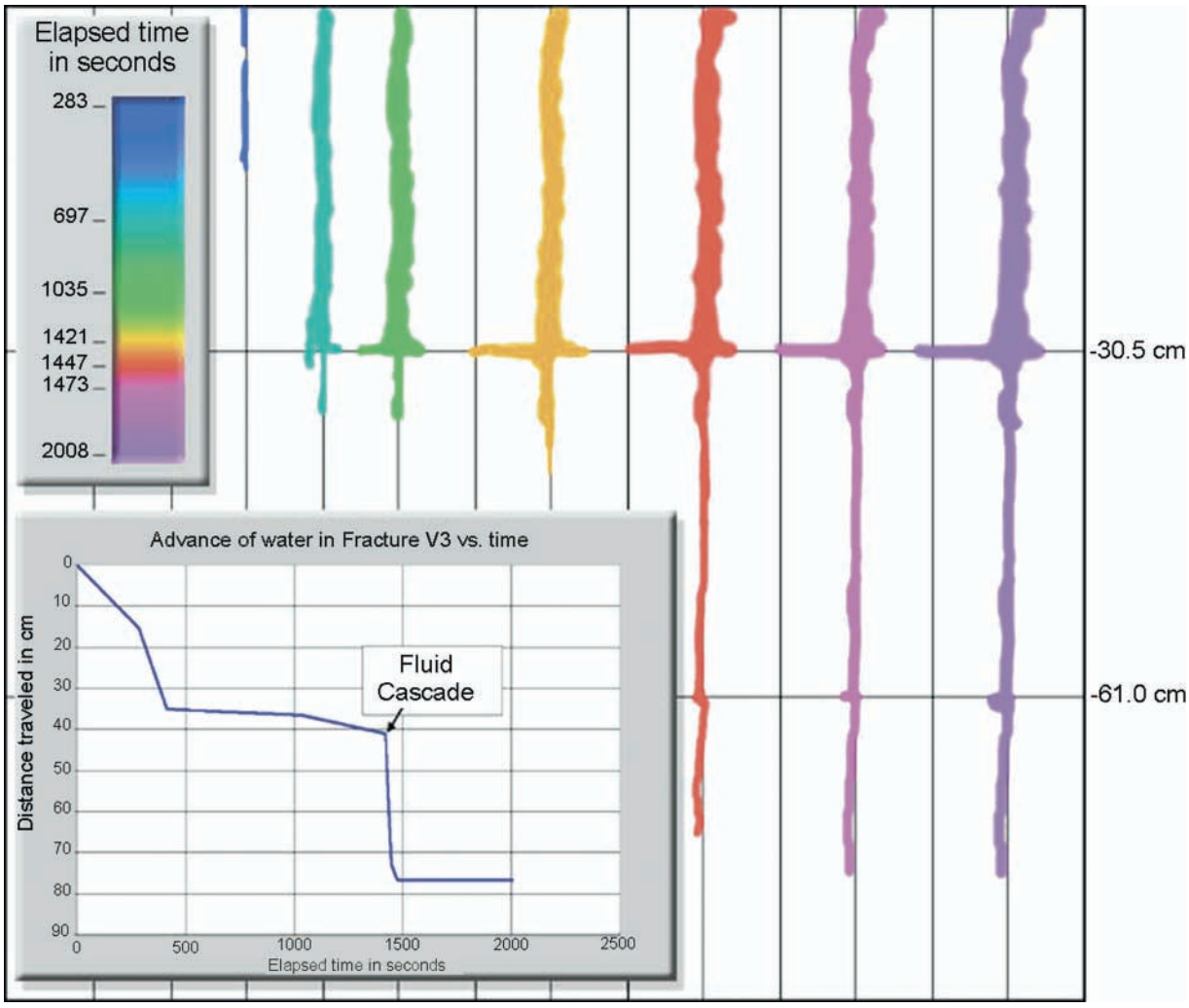

Fig. 5. Wetted structure development and a fluid cascade. The color images represent the development of the wetting pattern in Fracture V3 during Test 6. Individual colors represent the sequence of development at the indicated time. Water was retained at the fracture intersection of V3 and H2 between 413 and 1421 s (1008 s). At 1447 s a fluid cascade was observed that traveled 32 cm in 26 s. Graph shows the advance of the tip of the wetted area in Fracture V3 vs. elapsed time in seconds; the fluid cascade can be seen as a large step at 1421 s.

the importance of inertial forces generated during the release of a fluid cascade.

While the formation of fluid cascades was most obvious during the initial advance of the wetting front through the dry network, it was also observed at later times when the blocks had imbibed significant amounts of moisture. We must note, however, that fluid cascades did not occur at every intersection, they did not always persist with time as noted above, and we did not always observe the reoccurrence of a fluid cascade at the same intersection under repeated tests.

In addition to the fact that individual flow paths were observed to vary from one test to the next for the constant stack tests, we noted that the percentage of wetted area (wetted area divided by the total area) varied from one test to the next. The percentage of wetted area also changed during a single test when compared with other tests. For instance, if one test began with a higher percentage of wetted area during early time steps it was not unusual for this same test to show less wetted area at later time steps when compared with other tests, or vice versa. Figure 6 is a plot that shows the percentage of wetted area vs. time for the four infiltration tests under constant aperture conditions (Tests 5–8). The switching of rank for wetted area between tests can be clearly seen in this figure.

SUMMARY AND CONCLUSIONS

From our experiments, we draw four main summary points:

Convergence of flow with depth. With uniform distribution of flow across the top of this fracture network, the occurrence of converging or focused flow is at least as statistically significant as the occurrence of uniform flow.

Flow pathway switching is a common, if not characteristic, behavior of unsaturated fractured rock networks. We observed many instances of pathway switching where discharge from one fracture would increase at the expense of another. The switching of flow from one pathway to another occurred either gradually or

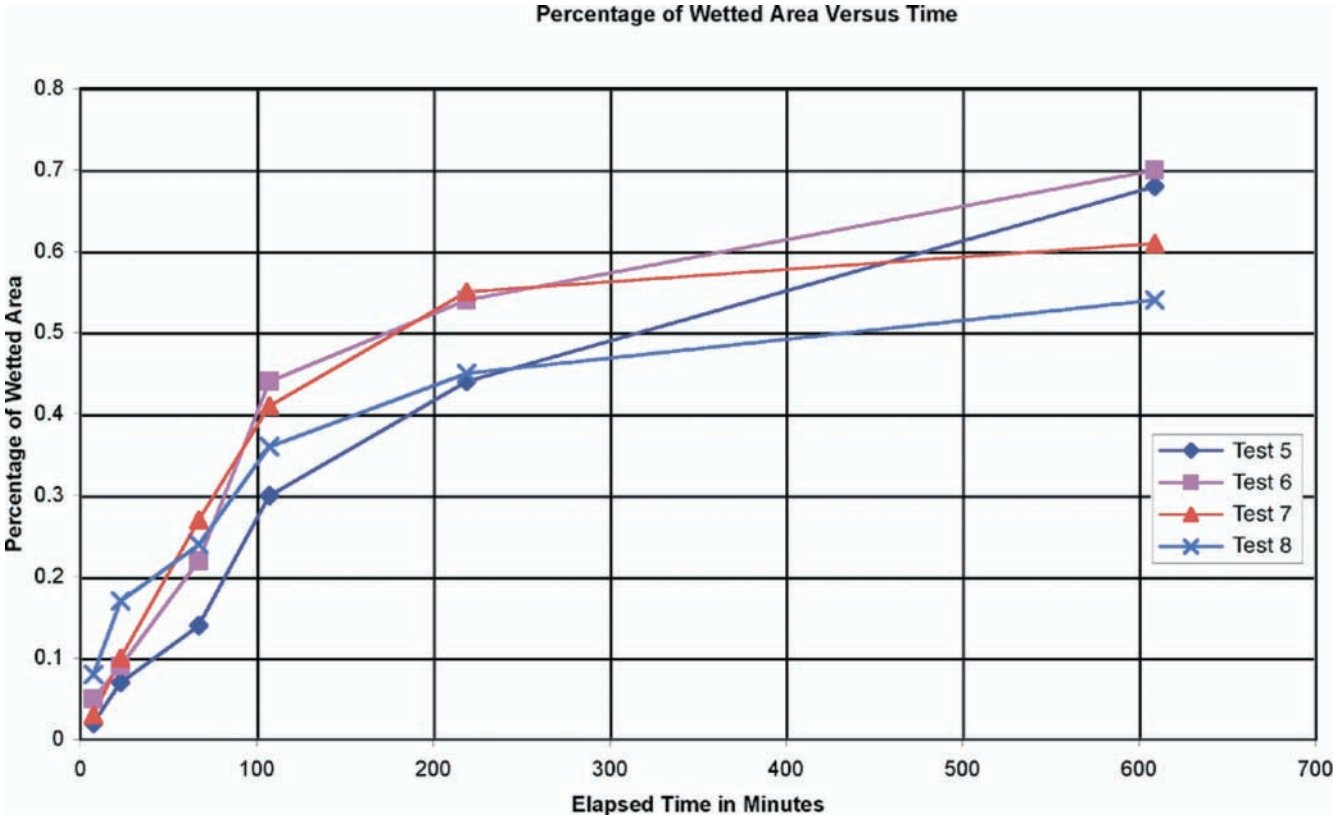

Fig. 6. Percentage of wetted area vs. time. Each line traces the percentage wetting through time (wetted area divided by total area) for each test.

abruptly. Periods of pathway switching (either gradual or abrupt) were more common than periods of steady, constant flow.

Fracture intersections act to accumulate and integrate the steady flux of vertically flowing water, generating less frequent, larger pulses of water. We observed water accumulating or pooling behind capillary barriers formed by intersections. The discharge of pooled water occurred in a fluid cascade as a critical point was exceeded. The capillary barriers formed by fracture intersections can divert vertically flowing water from one fracture into horizontal fractures, thus, increasing the pool volume relative to storage in a single fracture.

Wetting front pattern, including fluid cascades and stalled flow paths, and discharge flux to exit fractures with time were not repeatable for our experimental fracture network. We performed four tests to examine the repeatability of system behavior in a fractured rock network under similar wetting and initial moisture conditions. The results suggest that fractured rock systems do not exactly repeat wetting advance from one test to the next even under controlled laboratory conditions. The large variations in the observed flow patterns and discharge flux among these four tests seem to exceed what might be anticipated based on the small differences in test conditions.

Our tests yielded a number of significant observations and generate more unanswered questions. Of particular interest is the possibility that fluid cascades may span multiple intersections and grow to be quite large in natural fractured rock networks. With this possibility in mind, vadose zones consisting of fracture networks might harbor large multi-intersection "pools" that gather slow downward flow for long periods of time and then discharge abruptly in a fluid cascade quickly traversing large vertical distances.

The results of this experiment suggest that common modeling approaches cannot reproduce the behavior of the experimental results at this experimental scale. The results presented here add to the growing body of evidence calling for a paradigm shift in conceptualizing unsaturated flow in fractured rock vadose zones. Popular modeling approaches commonly applied to simulation of flow in fracture networks cannot duplicate the nonideal, dynamical behavior observed in our experiments (Fairley et al., 2001, 2004). Conceptualizing flow in fractured rock networks in a volume averaged manner, as commonly assumed, may be inappropriate in many situations. Significant variation in the location and flux of network discharge may occur without apparent external causes. Changes of internal intermediate flow pathways (switching) are at least as common as continuous flow along stable flow paths. The interaction of capillary and gravitational forces can trigger events that can rapidly transmit water significant distances. The convergence of flow with depth is probably a common feature in fracture networks.

ACKNOWLEDGMENTS

These experiments were conducted in 2001 and 2002 at the Fracture Flow Laboratory, INEEL, with support from the

INEEL Environmental Systems Research and Analysis Program, Office of Environmental Management, U.S. Department of Energy under DOE-ID Operations Office Contract DE-AC07-99ID13727. Data analysis and the writing of this manuscript were supported by the U.S. Department of Energy's Environmental Management Science Program under contract DE-AC07-99ID13727 with support from the U.S. Department of Energy's Basic Energy Sciences Geoscience Research Program under contract DE-AC07-99ID13727 at the INEEL and under contract DE-AC04-94AL85000 at Sandia National Laboratories. We would also like to thank Joe Lord and Raylene McMillin for their aid in constructing and maintaining the experiments, Paul Chiappini of Ziccardi Productions for help preparing visual images, and C.L. Reardon for measurements of microbial activity.

REFERENCES

Dahan, O., R. Nativ, M. Adar, B. Berkowitz, and Z. Ronen. 1999. Field observation of flow in a fracture intersecting unsaturated chalk. Water Resour. Res. 35:3315–3326.

Davidson, G.R., R.L. Bassett, E.L. Hardin, and D.L. Thompson. 1998. Geochemical evidence preferential flow of water through fractures in unsaturated tuff, Apache Leap. Appl. Geochem. 13:184–195.

Efron, B., and R.J. Tibshirani. 1993. An introduction to the bootstrap. Chapman and Hall, New York.

Fabryka-Martin, J.T., A.V. Wolfsberg, P.R. Dixon, S. Levy, J. Musgrave, and H.J. Turin. 1996. Summary report of chlorine-36 studies: Sampling, analysis and simulation of chlorine-36 in the Exploratory Studies Facility, Los Alamos National Laboratory. Report LA-CST-TIP-96-002. Los Alamos National Laboratory, Los Alamos, NM.

Fairley, J.P., T.R. Wood, and T.R. McJunkin. 2001. Comparison of numerical modeling results with laboratory experiments of flow in unsaturated, fractured rock. 2001 Fall meeting of the American Geophysical Union, San Francisco, CA. 10–14 Dec. 2001. AGU, Washington, DC.

Fairley, J.P., R.K. Podgorney, and T.R. Wood. 2004. Unsaturated flow through a small fracture–matrix network: Part 2. Uncertainty in modeling flow processes. Available at www.vadosezonejournal.org. Vadose Zone J. 3:101–108 (this issue).

Faybishenko, B., C. Doughty, M. Steiger, J.C.S. Long, T.R. Wood, J.S. Jacobsen, J. Lore, and P.T. Zawislanski. 2000. Conceptual model of the geometry and physics of water in a flow fractured basalt vadose zone. Water Resour. Res. 36:3499–3520.

Faybishenko, B.A., R. Salve, P. Zawislanki, K.H. Lee, P. Cook, B. Freifeld, K. Williams, and C. Doughty. 1998. Ponded infiltration test at the Box Canyon site: Data report and preliminary analysis. Rep. LBNL-40183. Lawrence Berkeley Natl. Lab., Berkeley, CA.

Faybishenko, B.A., P.A. Witherspoon, C. Doughty, T.R. Wood, R.K. Podgorney, and J.T. Geller. 2001. Multi-scale investigations of liquid flow in a fractured basalt vadose zone. *In* D.D. Evans et al. (ed.) Flow and transport in fractured rocks. 2nd ed. Geophysical Mono. 42. American Geophysical Union, Washington, DC.

General Accounting Office. 1998. Nuclear waste: Understanding of waste migration at Hanford is inadequate for key decisions. Report to Congressional Requesters. GAO/TCED-98-80. March 1998. GAO, Washington, DC.

Glass, R.J., M.J. Nicholl, S.E. Pringle, and T.R. Wood. 2002a. Unsaturated flow through a fracture-matrix network: Dynamic preferential pathways in meso-scale laboratory experiments. Water Resour. Res. 38(12):1281 doi: 10.1029/2001WR001002.

Glass, R.J., M.J. Nicholl, A.L. Ramirez, and W.D. Daily. 2002b. Liquid phase structure within an unsaturated fracture network beneath a surface infiltration event: Field experiment. Water Resour. Res. 38(10):1199 doi: 10.1029/2000wr000167.

Glass, R.J., M.J. Nicholl, and V.C. Tidwell. 1995. Challenging models for flow in unsaturated, fractured rock through exploration of small scale processes. Geophys. Res. Lett. 22:1457–1460.

Glass, R.J., M.J. Nicholl, and V.C. Tidwell. 1996. Challenging models for flow in unsaturated, fractured rock through exploration of small scale processes. SAND95-1824. Sandia National Laboratories, Albuquerque, NM.

LaViolette, R.A., R.J. Glass, T.R. Wood, T.R. McJunkin, K.S. Noah, R.K. Podgorney, R.C. Starr, and D.L. Stoner. 2003. Convergent flow observed in a laboratory-scale unsaturated fracture system. Geophys. Res. Lett. 30(2):1083 doi: 10.1029/2002GL015775.

Nicholl, M.J., and R.J. Glass. 2002. Field investigation of flow processes associated with infiltration into an initially dry fracture network at Fran Ridge, Yucca Mountain, Nevada: A photo essay and data summary. SAND2002-1369. Sandia National Laboratories, Albuquerque, NM.

Nicholl, M.J., R.J. Glass, and H.A. Nguyen. 1993. Small-scale behavior of single gravity-driven fingers in an initially dry fracture. p. 2023–2032. *In* Proc. Fourth Annual International Conference on High Level Radioactive Waste Management. 26–30 Apr. 1993. American Nuclear Society, Las Vegas, NV.

National Research Council. 2000. Research needs in subsurface science. National Research Council, Board on Radioactive Waste Management Water Science and Technology Board, National Academy Press, Washington, DC.

Podgorney, R.K., T.R. Wood, B.A. Faybishenko, and T.M. Stoops. 2000. Spatial and temporal instabilities in water flow through variably saturated fractured basalt on a 1-meter field scale. *In* B. Faybishenko et al. (ed.) Dynamics of fluids in fractured rocks. Geophys. Mono. 122. American Geophysical Union, Washington, DC.

Su, G.W., J.T. Geller, K. Pruess, and F. Wen. 1999. Experimental studies of water seepage and intermittent flow in unsaturated, rough-walled fractures. Water Resour. Res. 35:1019–1037.

Wood, T.R., D. Bates, C.W. Bishop, G.L. Heath, J.M. Hubbell, L.C. Hull, R.M. Lehman, S.O. Magnuson, E. D. Mattson, J.M. McCarthy, I. Porro, P.D. Ritter, M. Roddy, J.B. Sission, and R.P. Smith. 2000a. Deficiencies in vadose zone understanding at the Idaho National Engineering and Environmental Laboratory. INEEL/EXT-99-00984. INEEL, Idaho Falls, ID.

Wood, T., and B. Faybishenko. 2000. Large-scale field investigations in fractured basalt in Idaho: Lessons learned, Case Study to Chapter 3. p. 396–405. *In* B. Looney and R. Falta (ed.) Vadose zone science and technology solutions. Battelle Press, Columbus, OH.

Wood, T.R., B. Faybishenko, T.M. Stoops, C. Doughty, and J. Jacobsen. 1997. A conceptual model of tracer transport in fractured basalt: Large scale infiltration test revisited. Presented at the 1997 Geological Society of America Annual Meeting, Salt Lake City, UT. October 1997. GSA, Boulder, CO.

Wood, T.R., M.J. Nicholl, and R.J. Glass. 2002. Fracture intersections as integrators for unsaturated flow. Geophys. Res. Lett. 29(24):2191 doi: 10.1029/2002GL015551.

Wood, T.R., and G.T. Norrell. 1996. Integrated large-scale aquifer pumping and infiltration tests, groundwater pathways OU 7-06. Summary Rep. INEL-96/0256. Lockheed Martin Idaho Technologies Company, Idaho Falls, ID.

Wood, T.R., and R.K. Podgorney. 1999. Observations of water movement in variably saturated fractured basalt and its possible implications on advective contaminant transport. *In* Proc. Dynamics of Fluids in Fractured Rocks: Concepts and Recent Advances, International Symposium in Honor of Paul A. Witherspoon's 80th Birthday, Berkeley, CA. 10–12 Feb. 1999. Lawrence Berkeley National Laboratory, Berkeley, CA.

Wood, T.R., R.K. Podgorney, and B. Faybishenko. 2000b. Small scale field tests of water flow in a fractured rock vadose zone, Case Study to Chapter 3. *In* B. Looney and R. Falta (ed.) Vadose zone science and technology solutions. Battelle Press, Columbus, OH.

Wood, T.R., D. Stoner, C. Tolle, J. James, D. Peak, B. Faybishenko, and J. Crepeau. 2000c. Can a fractured basalt vadose zone be characterized as a complex system? *In* Summit 2000, Abstracts with Programs. Geological Society of America, Annual Meeting and Exposition, Reno, NV. Vol. 32, No. 7. 9–18 Nov. 2000. GSA, Boulder, CO.